Multi-sensor Personal Navigator Supported by Adaptive Knowledge Based System: Performance Assessment

S. Moafipoor, D.A. Grejner-Brzezinska and C. K. Toth
Satellite Positioning and Inertial Navigation (SPIN) Laboratory
The Ohio State University

Abstract-**The prototype of a personal navigator, which integrates Global Positioning System (GPS), tactical grade inertial measurement unit (IMU), digital barometer, magnetometer, and human pedometry to support navigation and tracking of military and rescue ground personnel has been developed at The Ohio State University Satellite Positioning and Inertial Navigation (SPIN) Laboratory. This paper discusses the design, implementation and performance assessment of the prototype, with a special emphasis on dead-reckoning (DR) navigation supported by a human locomotion model. The primary components of the human locomotion model are step frequency (SF), extracted from GPS-timed impact micro-switches placed on the shoe soles of the operator, step length (SL), and step direction (SD), both determined by predictive models derived by the adaptive knowledge based system (KBS). SL KBS is based on Artificial Neural Networks (ANN) and Fuzzy Logic (FL), and is trained a priori using sensory data collected by various operators in various environments during GPS signal reception. An additional KBS module, in the form of a Kalman Filter (KF), is used to improve the heading information (SD) available from the magnetometer and gyroscope under GPS-denied conditions, as well as to integrate the DR parameters to reconstruct the trajectory based on SL and SD. The current target accuracy of the system is 3-5 m CEP (circular error probable, 50%). This paper provides a performance analysis in the indoor and outdoor environments for two different operators. The system's navigation limitation in DR mode is tested in terms of time and trajectory length to determine the upper limit of indoor operation before the need for re-calibration.**

1. INTRODUCTION

The main objective of the prototype of a Personal Navigator (PN) developed at The Ohio State University Satellite Positioning and Inertial Navigation (SPIN) Laboratory is to provide an accurate and reliable portable navigation device for localizing ground personnel in various environments, such as combat and emergency situations, with a target performance of 3-5 m CEP (circular error probable, 50%). This PN is a multimodal device, working in absolute GPS/IMU mode, or in a Dead Reckoning (DR) mode, depending on the GPS (Global Positioning System) signal availability. It consists of a range of self-contained sensors, including GPS, IMU (inertial measurement unit), digital barometer, magnetometer, and human pedometry model [1-2]. The human body is considered here as a sensor, capable of providing information that can be converted to location coordinates by using the corresponding models and navigation algorithms. All sensors require precise calibration during GPS availability, in order to support the estimation of parameters required for DR navigation, including direction, walking distance and altitude.

The potential of the self-contained sensors in representing DR parameters was reported by, e.g. [1-5], together with the initial performance analysis of the DR navigation supported by the human locomotion model. The human locomotion model is focused on analyzing measurable parameters, such as step interval or step frequency (SF), step length (SL), step direction (SD), locomotion pattern, etc. for each step. To properly capture the SL of a mobile user in a variety of environments and dynamics, and to assure that, if needed, the type of motion of the user can also be captured, two different modules of adaptive knowledge based system (KBS) based on (1) Artificial Neural Networks (ANN), and (2) Fuzzy Logic (FL) have been implemented [5-7].

Since the DR navigation performance is largely governed by the KBS, its training and updating should be performed not only prior to the mission, but also along the navigation trajectory, whenever possible. This matter is more important for SD modeling, because any error in SD estimation, even for a single step, could cause an immediate drift of the navigation trajectory. The focus of this paper is on the performance assessment of the DR navigation system based on the KBS implementation and on the methods of improving the modeling/prediction process of SL and SD parameters. Furthermore, the performance assessment will attempt to determine, based on the field data available to date, the upper limit of DR navigation within the target threshold of 5m CEP, especially for indoor operational environments, where the entire system is subject to a substantial amount of ambient perturbation factors. To this end, a performance analysis example is provided in the indoor and outdoor environments.

The paper is structured as follows: Section 2 is an overview of the PN system in terms of hardware configuration. Section 3 illustrates the operational modes of the PN. Section 4 discusses the KBS design and its contribution to estimating the DR parameters. The performance analysis of the DR navigation is presented in Section 5. Finally, the summary and conclusions are presented in Section 6.

2. OVERVIEW OF THE PN HARDWARE CONFIGURATION

Fig. 1 shows the PN prototype in a backpack configuration. A dual-frequency Novatel GPS antenna connected to an OEM4 receiver is placed on a pole, sufficiently far from the operator's body; the inertial navigation is furnished by a tactical grade Honeywell HG1700 IMU.

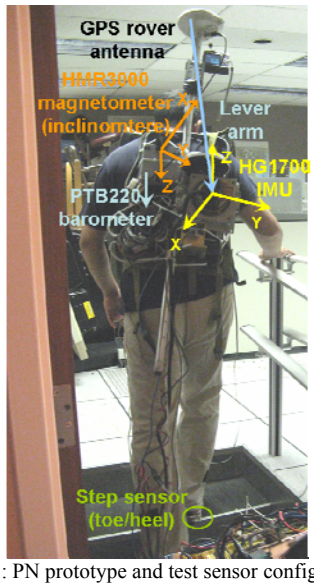

Fig. 1: PN prototype and test sensor configuration

The lever arm, i.e., the distance from the phase center of the GPS antenna to the center of IMU, was carefully measured and accounted for in the GPS/IMU Extended Kalman filter (EKF). The IMU orientation is as follows: the X-axis is aligned opposite to the direction of motion; the Y-axis points across the direction of motion, and the Z-axis points towards the "up" side of the YZ plane. The Honeywell HMR3000 magnetometer (inclinometer/compass) measures the absolute orientation through a combination of three orthogonally-aligned magnetic sensors which measure the Earth's magnetic field intensity and two orthogonally-aligned tilt sensors which measure the direction of gravity. The HMR3000 magnetometer is mounted in a predefined orientation with respect to the IMU axes; note that if the systems are not collocated properly, the misalignment between the two sensors should be introduced into the state vector of the EKF. In the configuration shown in Fig. 1, the X-axis of the magnetometer is aligned with the direction of operator's motion, and the Y-axis is aligned with the cross-direction of operator's motion. The Vaisala PTB220 digital barometers used in the prototype can be fine-adjusted and calibrated against pressure standards that have high accuracy and stability as well as known traceability to international standards. This sensor, after the initial calibration, can estimate the altitude with accuracy better than ±1.5 m (1-sigma).

The primary sensor that allows easy determination of step events is a set of four GPS time-synchronized micro-switches, located in the shoe soles (at heels and toes; see Fig. 1), which are used to sense impact, i.e., the instants when the operator's shoes hit the ground. They can also be used as a reliable indicator of whether the operator is in motion or at rest (standing). Dual frequency GPS data (carrier phase and/or pseudorange), raw IMU data and other sensory data are processed by the EKF in a tight integration mode. To facilitate the redundancy in the navigation solution, particularly in the DR mode, the multisensor PN configuration is completed by utilizing the human dynamics-based model, as an auxiliary sensor.

3. PN OPERATIONAL MODES

The multisensor PN system runs in three operational modes, as shown in Fig. 2. First is the initial calibration mode, which includes the magnetometer's autocalibration step and GPS-based calibration of the other sensors.

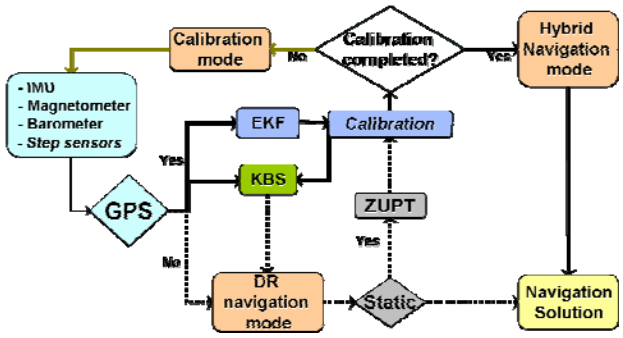

Fig. 2: PN system and operational modes: (1) calibration (initial calibration), (2) hybrid navigation, (3) DR navigation

Once the calibration is complete, the system enters the second mode – hybrid navigation. Although in this mode the system still keeps calibrating the self-contained sensors, the main calibration task is to train the KBS, as long as GPS signals are available, in order to support navigation in GPS-denied conditions. With the loss of GPS, the system switches to the DR navigation mode. Starting from a known position before the GPS outage, the successive position displacements are accumulated. The DR parameters are determined by the predictive models, derived by the KBS during the hybrid navigation period. Upon the reacquisition of GPS signals, the system switches back to the hybrid navigation mode. Furthermore, any stationary period can be utilized for a partial sensor calibration in the ZUPT (zero velocity update) mode (see, e.g., [8]). A detailed description of different operational modes is presented next.

A. Calibration Mode

The state vector of the tightly coupled EKF includes 3 position errors, 3 velocity errors, 3 attitude component errors, 3 accelerometer biases and 3 scale factors, 3 gyro biases and 3 scale factors, as well as 2 barometer and 6 compass magnetometer (inclinometer) errors. Fig. 3 shows the EKF design architecture together with the type of observations obtained from each sensor.

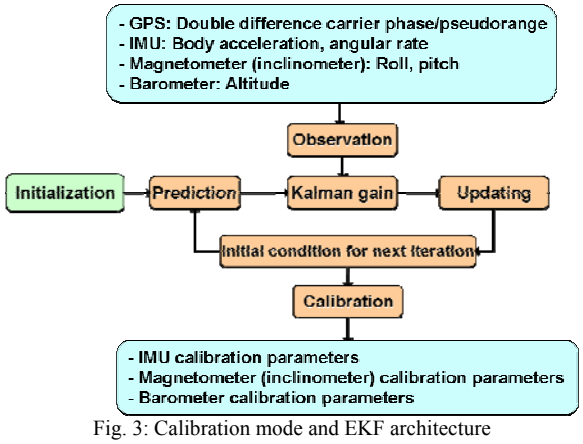

Fig. 3: Calibration mode and EKF architecture

As far as the EKF is concerned, the first and most important task is to calibrate the IMU sensors, until the filter reaches the steady state and is ready to navigate. The error states of the barometer and magnetometer's inclinometer are also included in the EKF state vector, and their epoch-by-epoch estimators are used to calibrate the tilt (roll/pitch) and height measurements. At the initial calibration mode stage, the magnetometer compass heading is separately calibrated by the autocalibration process (see, e.g., [9]). Later, in the hybrid navigation mode, its calibration parameters are included in the EKF state vector.

The GPS positioning solution (or the GPS/IMU solution) interpolated for the micro-switch time events of pre-planned calibration maneuvers can provide accurate training and, therefore, calibration for the SL KBS.

B. *Hybrid Navigation Mode*

Once the sensors are calibrated and the EKF has reached the steady state, the system enters the hybrid navigation mode. The general structure of the hybrid navigation system mode is shown in Fig. 4. Within this structure, two interconnected procedures are performed as a byproduct of the navigation solution: (1) updating the sensor calibration parameters and recording the last calibration sets, and (2) training the KBS system supporting the human locomotion modeling.

The basis for DR navigation in the PN system is formed by the KBS associated with the human locomotion model designed for accurate prediction of the SL of a mobile user, and an adaptive calibration of gyro and magnetometer to provide SD. In addition, the KBS can determine the overall dynamic locomotion pattern, by which the navigation trajectory can be reconstructed more consistently. Later, in the absence of GPS signals, the data streams from the remaining sensors are corrected based on the last recorded calibration parameters, and sent to the KBS module for prediction of DR navigation parameters.

C. *DR Navigation Mode*

The DR navigation in this project, as shown in Fig. 4, is achieved through the following tasks: (1) step detection with the micro-switches, located in the shoe soles, synchronized with GPS time; (2) KBS–based SL prediction; (3) KBS-based SD determination; and (4) KBS-based DR trajectory reconstruction.

Two approaches, based on ANN and FL, have been implemented for SL modeling [5,7]. The main reason behind using the computational intelligence techniques to represent the SL model, is due mainly to the complexity as well as limitations of the existing quantitative techniques for human locomotion modeling. On the other hand, the SD can be measured directly by the magnetometer compass and/or gyro. Therefore, the problem of SD determination is not in its modeling, but in finding a reliable approach to calibrate the compass/gyro sensors. During GPS signal reception, the EKF estimates the gyro errors to ensure the attitude accuracy. The continuous correction of these errors assures a long-term accuracy for heading estimation.

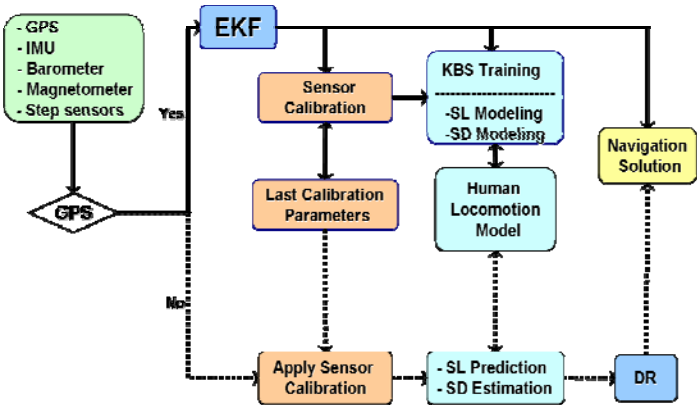

Fig. 4: Hybrid navigation supporting system calibration and KBS training.

However, long GPS gaps may cause gyro drift growth, and thus, an increase of attitude error. In such a case, if the vertical gyro's drift exceeds the level of the magnetometer compass errors, the system switches to the magnetometer compass solution, which is rectified by the last calibration parameters before the GPS outage.

Two approaches have been considered for magnetometer compass calibration: (1) an autocalibration [9], and (2) a dynamic calibration (*ibid*). In *ibid*, two approaches were proposed for dynamic calibration during the GPS signal reception: first, based on multisensor Kalman filtering and second, based on the ANN approach. For real-time magnetometer calibration in this paper, the magnetometer is initially calibrated utilizing an autocalibration procedure. Then the magnetometer compass output is modeled and updated by the reference solution from the calibrated gyro. It is expected that the calibrated magnetometer heading can improve the reliability of the SD determination by bridging the gaps when the gyro errors are excessive, provided that no significant magnetic disturbances occur.

To integrate the KBS associated with human locomotion model, an additional module is used to improve DR navigation mode, which will be addressed in the next section.

4. KBS-BASED DR PARAMETER ESTIMATON

In the PN system described here, the locomotion pattern is determined by analyzing the magnitude of the acceleration of each step, its standard deviation, maximum-minimum values of acceleration, and the angular velocity obtained from the gyroscope. These values are passed from a pre-defined fuzzy engine, and the output is the locomotion pattern in terms of standing, crawling, stumbling, walking, jogging, running, sprinting, and climbing stairs [7]. Alternatively, the ANN approach can be used, where sensory data provide an input to the pre-calibrated ANN that provides the SL prediction based on the past knowledge and the current data (see, e.g., [10]).

A. *SL Modeling*

To parameterize the SL specific for a particular locomotion pattern (in FL-based approach), or as a function of specific measurable parameters (in ANN approach), a set of variables is extracted from the sensors, as shown in Fig. 5, for each step separately.

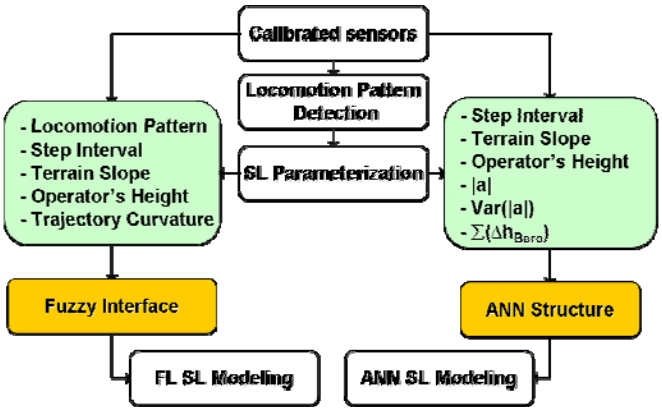

Fig. 5: SL parameterization in FL and ANN approaches

Then, according to the type of the model (ANN/FL), a corresponding KBS is used to process the information according to the KBS module design and parameterization requirements. Although the parameters used for ANN SL modeling are likely to be different from those used for the FL-based SL model, both parameterizations represent similar information content. For example, the locomotion pattern parameter, which is separately determined in the FL approach, can be inferred from the ANN structure. In the FL SL modeling, the expert who analyzes the parameterization data, defines the generic rules in the form of membership functions for SL modeling. To ensure that the defined generic rules cover the output responses, numerous factors that impact the SL modeling, some of which independent of the individual operator, and others operator-dependent, such as operator's height, must be considered.

Furthermore, the impact of the operating environments and other physical dynamic factors on the defined rules, such as trajectory curvature or surface type and its topography, should be taken into account. Operators typically move faster on straight parts of the trajectory, as compared to the curved sections, with the speed differences proportional to the curvature of the path. As a result, in the FL SL modeling, the SL function is parameterized by the following parameters: locomotion pattern, step interval, terrain slope, operator's height, and trajectory curvature. These are the most essential parameters that govern the FL SL modeling in our design. However, due to the open-ended architecture of the FL structure, the system can be optimally tuned for additional types of locomotion patterns or additional rules that are not yet addressed in our implementation.

In comparison to the FL SL modeling, the main advantage of the ANN method is that the mapping between SL parameterization data and SL training is done automatically. In this project, a Radial Basis Function (RBF) ANN is used [3,5,11]. The RBF network is designed to perform input-output mapping based on the concept of a locally tuned and overlapping receptive field structure. The RBF network is basically trained by the hybrid learning rule, unsupervised learning in the input layer (e.g., the parameterized data listed in Fig. 5), and supervised learning in the output layer (i.e., SL).

Another advantage of the ANN approach is that the KBS-training can be performed simultaneously with the GPS data logging. However, for better tuning of the system, it is necessary that the user performs a variety of walking patterns with different speeds and in different environments. Thus, each experiment performed by an operator provides modeling data that are recorded in the ANN SL-database. Once the database has been created based on the past and current training datasets, the RBF network is ready to predict the SL value based on the actual sensory data. If the RBF network is trained with only a certain type of training datasets, then the accuracy of the estimated SL value will be restricted by the incomplete training experience [12].

B. SD Determination

The SD in the PN system is directly observed by at least two sensors: the HG1700 gyro and the HMR3000 magnetometer compass. However, considering the stability of each of the sensors, different approaches are presented in this paper. For HG1700 gyro, (1) shows the differential equation that must be integrated over time to obtain the attitude angles:

$$\begin{pmatrix} \dot{\eta} \\ \dot{\chi} \\ \dot{\alpha} \end{pmatrix} = \begin{pmatrix} 1 & \sin\eta\tan\chi & \cos\eta\tan\chi \\ 0 & \cos\eta & -\sin\eta \\ 0 & \sin\eta\sec\chi & \cos\eta\sec\chi \end{pmatrix} \left(\omega_{ib}^{b} - C_{n}^{b}\omega_{in}^{n} \right) \qquad (1)$$

where, η, χ, α are roll, pitch, and heading angles, respectively, ω_{ib}^{b} is the gyro output, C_{n}^{b} is the direction cosine matrix that transforms the navigation frame (*n*-frame) to the body-fixed frame (*b*-frame), and ω_{in}^{n} is the rotation rate vector of the *n-frame* with respect to the inertial frame *(i*-fame), coordinated in the *n*-frame [13]. In the PN system, the initial conditions for this equation are established from the last epoch before the GPS outage occurred.

The gyro attitude is extremely sensitive to the gyro drift error, $\delta\omega_{ib}^{b}$. The HG1700 IMU, with the gyro stability better than 3-5º/hr, is sufficiently reliable to provide SD for a limited time during GPS outages, especially after tuning the filter, but eventually the size of the gyro drift necessitates recalibration (the duration of an acceptable solution depends on the state of gyro calibration before the GPS outage).

If, due to GPS-denied conditions, the gyro drift is not compensated during the navigation task, the PN system uses the magnetometer compass to determine the SD value, as already mentioned. The HMR3000 magnetometer compass operates based on sensing and measuring the Earth's magnetic field. If the magnetometer were aligned with the local horizontal plane, the heading, α, would be calculated as α =atan2 (H_y, H_x); where, H_x and H_y represent the horizontal magnetic field components of the Earth. To rotate the measured magnetic components to the horizontal plane, the HMR3000 is equipped with a two-axis tilt sensor, thus, the combination of the tilt sensor and the magnetometer sensor can measure the entire set of three attitude angles.

Since a magnetometer compass operates based on sensing and measuring the Earth's magnetic field, it is very sensitive to any ferrous materials close to the sensor. These materials superimpose an extra magnetic field, causing heading deviation. This deviation is usually adjusted by introducing a shift and a scale factor, as shown in (2), along the horizontal axes of the sensed magnetic field.

$$\alpha = \text{atan2}\left(S_y H_y + b_y, S_x H_x + b_x\right) \quad (2)$$

where S_x, S_y are two scale factors, and b_x, b_y are two biases along the horizontal axes of the sensed magnetic field. These parameters should be estimated by the autocalibration procedure performed in the calibration mode, independent from EKF structure. Once the calibration mode is completed, the system automatically enters the hybrid navigation mode, while the four magnetometer calibration parameters are saved and used as constant scale and bias terms used to estimate the heading from the magnetic field vector, as shown in (2). However, as the mobile user moves along, the environment around him changes, and it is possible that the surrounding ferrous materials will cause some deviations of the magnetometer. Deviations may range from a few degrees in the outdoor environments to tens of degrees in the indoor environments. Consequently, a real-time recalibration is required to adjust the bias and scale factor parameters to the new magnetic field, on the basis of a reference solution provided by the calibrated gyro (if available). Two different approaches can be considered.

The first logical approach is to keep updating the magnetometer calibration parameters based on reference directions, provided by the calibrated gyro (or any other external reference direction coming from e.g., map data, such as hallway layout and direction). For this purpose, (2) can be linearized with respect to the magnetometer calibration parameters, S_x, S_y, b_x, b_y, which can be estimated by the batch least squares method. However, this approach requires an iterative process on a batch of data, and thus, it cannot be performed in real time [14]. Still missing in this study is an appropriate algorithm to convert the model into a non-iterative least squares solution, where the unknowns can be estimated by a sequential process suitable for real-time implementation in the main navigation EKF structure [15].

In the second approach, to accommodate the possible magnetic disturbances of the local area, the magnetometer (compass) heading, rectified by the four pre-calibrated parameters, as explained above, is modeled by:

$$\psi_k = \lambda_c \alpha_k + b_c + e \quad (3)$$

where, ψ_k is the calibrated gyro heading at time k, α_k is the measured compass heading (2), λ_c is the compass scale factor, b_c is the compass bias (local magnetic disturbance), and e is the observation error. The bias factor can be considered as the effect of the soft and hard magnetic disturbances. As a result, the EKF is augmented by 2 additional states, representing the compass bias and scale factor, to let the filter jointly estimate the local magnetic field disturbance and update the compass heading. In the current implementation, the gyro observation noise variance is set to $(0.1^\circ)^2$, which is much smaller than the magnetometer compass heading accuracy, 1º. Therefore, the GPS/IMU/magnetometer compass solution is largely governed by the increased weight assigned to the gyro rate measurements.

As a conclusion, during GPS reception, the gyro is continuously calibrated, and its heading is used to update the calibration parameters of the magnetometer compass. In the absence of GPS signals, three different methods are possible for determining the SD value (a numerical example of these three different heading solutions is shown in Fig. 8). In the first method, the rate gyro heading is integrated over time, assuming that the gyro drifts do not change during the integration period; however, the duration of an acceptable gyro heading depends on the quality of gyro and the state of gyro calibration. If gyro drift is not compensated for a long time due to calibration instability, the magnetometer compass heading is used instead. But the magnetometer compass heading can be also deflected by the uncompensated magnetic disturbances in the changing environment as the operator moves along the trajectory. In the third approach, the heading solution is provided by the integration of gyro and magnetometer through the same EKF that is used for multisensor integration in the calibration and hybrid navigation modes. This solution is derived on the basis of the last calibration parameters applied to the gyro and magnetometer compass measurements (as shown Fig. 4). However, during a prolonged absence of GPS signals, all heading solutions will be degraded due to the lack of updated calibration parameters for both gyro and magnetometer, resulting in an unacceptable level of navigation errors. So, a quality control/quality assurance (QA/QC) mechanism should be designed to determine when the quality of the gyro and magnetometer heading solutions become unacceptable. This is a subject of our current investigation.

The QA/QC mechanism based on the gyro heading threshold is inversely proportional to the stability of the gyro bias drift. Furthermore, since the gyro drift depends on both the temperature and the dynamic rate [13], trajectories with many sharp turns and high dynamic rates, will result in a higher gyro drift, which should be accounted for in evaluating the quality of the gyro heading. While the gyro drifts with time and dynamics, the calibration parameters of the magnetometer are location dependent. As a result, any quality control mechanism for the magnetometer compass is associated with monitoring the intensity of the magnetic field. If the magnetic flux density at the current location is principally different from its counterpart at the location of calibration, the quality of the magnetometer compass may not be considered acceptable. Further development of the QA/QC mechanism for the heading solution and to ensure better process control, more flexibility and more reliable SD determination is currently under way.

C. DR Trajectory Reconstruction

With heading, α (SD), measured by the gyro and/or magnetometer and the pre-calibrated SL, predicted by the KBS, the DR position of the next point on the trajectory (see Fig. 6) can be determined, as shown in (4):

$$\begin{cases} x_{k+1} = x_k + SL_k \sin(\alpha_k) \\ y_{k+1} = y_k + SL_k \cos(\alpha_k) \end{cases} \quad (4)$$

But this kind of point-to-point navigation trajectory reconstruction has significant shortcomings, particularly in its inability to accommodate outlier detection, since no continuity/predictive model for the trajectory is formed. Outliers can be caused e.g. by imprecise SL prediction and uncalibrated magnetometer/gyro SD determination, which can easily bias the determination/evaluation of the subsequent positions. Moreover, the SL and SD prediction, derived from KBS, contain random errors. The accumulation of these errors causes deviation in the trajectory over time. It was observed that in the indoor environments, the subsequent SD values would "jump" by tens of degrees. In addition, the SL and SD values for each step are predicted independently, without any physical interpretation, which is a serious disadvantage. An approach that can address these shortcomings is the consideration of the human body model, which can facilitate access to the mechanism of human motion. Ref. [16] showed that human motion demonstrates specific characteristics which make the definition and the identification of generic models of human motion feasible.

To find the correlation between successive SL parameters, three scenarios can be considered: (1) random fluctuations; (2) Gauss Markov processes (GMP); and (3) locomotion-dependent processes. The simplest explanation for the point-to-point variations in the walking rhythm is that step-by-step SL represents an uncorrelated (white) noise superimposed on a basically regular process. A second possibility is that these fluctuations have short-range correlations, such as a GMP with an exponential decay of the system. A third, more intuitive possibility is that the fluctuations in the SL could exhibit some type of locomotion pattern, superimposed on other scale-free, uncorrelated or GM process.

In the last case, it is assumed that the SL from one point to the next changes according to the locomotion pattern variation. If the locomotion pattern does not change during the movement, the fluctuations are in the range of random white noise with a pre-defined variance. If the locomotion pattern changes gradually, e.g. from normal walking to fast walking, a GMP can be applied. As the locomotion pattern switches from walking into running, the kinematics of locomotion change abruptly, and therefore an uncorrelated noise can be considered. Applying such knowledge to the DR navigation not only assures correlation between successive SL values, but also improves the system's performance by rejecting the outliers in predicted SL.

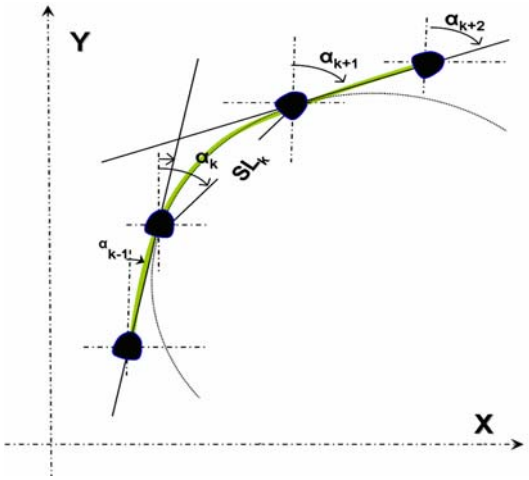

Fig. 6: DR trajectory reconstruction

Similarly to the framework applied to SL modeling, the SD parameters, obtained from magnetometer/gyro, can also be supervised (or controlled) on the basis of generic models of human motion. For instance, the SD can be predicted using a Bayesian framework, which has also been developed for DR trajectory reconstruction based on probabilistic modeling of operator's position [17]. To facilitate the prediction model, the SD is parameterized into heading and heading rate. As shown in (5), the SD parameter observed at the current epoch, *k*, can be predicted by two primary inputs: the SD value at the previous epoch, α_{k-1}, and the heading rate, $\dot{\alpha}_k / 2$ that expresses the average change of heading between two consecutive steps.

$$SD_k = \alpha_{k-1} + \frac{\dot{\alpha}_k}{2} \Delta t_k \quad (5)$$

The heading rate can be predicted by the locomotion pattern. For example, when an operator is running, the heading rate is small because, on the basis of human locomotion model, there is less chance for a runner to change his direction abruptly. Similarly, during the climbing of a single flight of stairs, the heading rate does not change considerably.

Applying such knowledge to advance the integrity of the system produces a framework which exploits statistical models which characterize the human locomotion model. This framework also provides a principled probabilistic model to combine DR parameters, predicted SL and SD, and to introduce *a priori* knowledge related to the locomotion pattern of operators to detect and track during the navigation task. Thus, a KBS in the form of a Kalman filter, separate from the navigation/calibration EKF, referred to as DR-KF, is proposed to model the DR parameters. The DR-KF uses the KBS algorithm for the purpose of: (1) predicting SL and SD models using locomotion pattern, (2) updating SL and SD values, and (3) reconstructing the DR trajectory. The implemented Kalman filter includes five unknowns: SL, heading rate, SD, and horizontal position coordinates. Equation (6) shows the general structure of the DR-KF, where the prediction model is established based on the body locomotion pattern (activity type):

If locomotion is [stumble/stand/walk/run/climb] THEN

$$\begin{cases} X_k = \Phi_k^{Activity} X_{k-1} + u_k^{Activity} \\ Z_k = H_k X_k + v_k \end{cases} \quad (6)$$

where X is the five parameter-state vector; $\Phi^{Activity}$ and $u^{Activity}$ are the transition matrix and the state vector error of the prediction model, respectively, calculated according to the current type of locomotion; Z is the observation vector, including KBS–based predicted SL and SD and the associated position coordinates, which are calculated by accumulating incremental motion along the last updated position coordinates; H is the observation matrix, H=[1 0 0 0 0; 0 0 0 0 0; 0 0 1 0 0; 0 0 0 1 0; 0 0 0 0 1], and v is the observation error, representing the uncertainties in estimating SD and predicted SL for each step.

A system where the prediction model changes because of a fuzzy rule (i.e., the class of body locomotion) is referred to as a Takagi-Sugeno-Kang (TSK) fuzzy inference model [18]. The main advantage of using the TSK fuzzy inference model for navigation trajectory reconstruction is that it allows for an easy combination of various behaviors (rules) through a command fusion process, instead of using fixed parameters for the entire process [19]. As an example, (7) shows the prediction modeling for walking activity. For a walking person, a first-order linear function is the simplest dynamic representation of DR trajectory prediction, while for jogging or running the higher-order models should be used. This assumes that the person keeps moving along a route, determined from the initial position, x_k, y_k, the SD_k (5), and the predicted SL_k.

$$\begin{cases} SL_k = SL_{k-1} + u_{SL} \\ \dot{\alpha}_k = \dot{\alpha}_{k-1} + u_{\dot{\alpha}} \\ \alpha_k = \alpha_{k-1} + \dot{\alpha}_{k-1}\Delta t_k + u_\alpha \\ \\ x_{k+1} = x_k + SL_k \sin(\alpha_{k-1} + \dfrac{\dot{\alpha}_k}{2}\Delta t_k) + 1/2\Delta t_k^2 a_k^x \\ y_{k+1} = y_k + SL_k \cos(\alpha_{k-1} + \dfrac{\dot{\alpha}_k}{2}\Delta t_k) + 1/2\Delta t_k^2 a_k^y \end{cases} \quad (7)$$

In (7), the SL_k and heading rate, $\dot{\alpha}_k$, are predicted as random constant models, with the uncertainty defined by $u_{SL}, u_{\dot{\alpha}}$, respectively. The SD (α_k) is predicted by a linear combination of the previous SD (α_{k-1}), the heading rate, as well as the step interval time, Δt_k. If the step interval is short, it indicates that the locomotion pattern is close to high dynamic locomotion, and therefore subject to, most probably, almost constant heading. The uncertainty in heading prediction, u_α, is proportional to the corresponding locomotion pattern. For low dynamic movement, this uncertainty can be increased to more than a few degrees, and for high dynamic, it can be limited to a few degrees. The uncertainty of trajectory propagation is defined by the random, time-varying horizontal acceleration components, a^x, a^y, and the square of the step interval time, Δt_k^2. As can be seen, for these statistical schemes, the key point is to provide appropriate statistical characterization, and focus on the definition of appropriate probabilistic models of dynamic information for human motion.

As a conclusion, a KBS is applied to the prediction model by assigning a different system noise error according to the locomotion pattern. Using the knowledge about the mechanism of walking in terms of SD and SL can be useful to adjust the estimations, particularly SD, and smooth the trajectory reconstruction. The observation model, including SD and SL measurements with the corresponding error models, updates the prediction model. The recursive structure of the DR-KF also estimates the covariance matrix, indicating the quality of the reconstructed trajectory. Furthermore, this scheme can convert the point-to-point DR navigation into a dynamic navigation. The DR-KF structure can also be extended to 3D, including altitude, and roll/pitch angles. In this case, the measurements coming from the barometer and magnetometer's inclinometer are added to the observation model.

5. SYSTEM PERFORMANCE EVALUATION

This section provides a performance evaluation of the prototype, with a special emphasis on DR navigation supported by the human locomotion model. The experiment started outdoor, in the calibration and subsequently, hybrid navigation mode, followed by the DR navigation indoor. The system performance based on adaptive KBS is primarily evaluated in terms of the quality of the navigation solution for a short trajectory in the confined environment. Then, the experiments are conducted to determine the navigation limitations in the DR mode in terms of the trajectory length and duration, to assess the upper limit of indoor operation before the additional calibration of the sensors, particularly gyro and magnetometer, is required.

For this purpose, a series of datasets was collected on August 21 and 26, 2007 at the Center for Mapping (CFM) single-storey building, The Ohio State University, with two different operators, S and E, respectively. The data collection procedure was almost identical for both operators on both days. In order to calibrate the system, the mobile users performed several maneuvers outside the CFM building. Although a full circle was sufficient to calibrate the magnetometer and barometer, two more loops followed to calibrate the IMU sensors. Afterwards, the users entered the building, walked the hallways of the center, and made several loops following the control points marked in the hallways. For more control, after each loop, the users stopped for one minute at a marked point with known coordinates.

The floor plan of the building was previously acquired by classical surveying methods, and several control points were established in the hallways to accuracy better than 1-2 cm in E and N, and 5 mm in height. The main objective of the control points was to facilitate the prediction of the user's position and provide control for the reference trajectory. All calibration demonstrations in this paper are based on double-difference carrier phase observations.

A. Online Calibration and Hybrid Navigation Performance

The main objective of the outdoor experiment was to test the performance of the KBS modules in SL and SD modeling. During GPS signal reception, the double-difference carrier phase observations in the EKF were used to calibrate HG1700 gyro and HMR3000 magnetometer, as already mentioned. The calibrated gyro heading, in fact, represents the reference solution, and therefore, the DR trajectory reconstruction associated by this type of SD solution only represents the impact of the SL error, which was earlier explored by e.g., [1-2]. Thus, the real system performance in DR mode for outdoor experiments must be demonstrated by the SD provided by the magnetometer compass, where two different scenarios can be considered to rectify the magnetometer compass heading: first, using the last calibration parameters based on (2); and second, using the last epoch-by-epoch calibration parameters based on (3). In this experiment, the second approach is chosen to determine the SD value. This approach also tests the dynamic reaction of the magnetometer calibration model to the change of magnetic field in the changing environment.

In addition, the existing ANN SL-database was activated for the operator S. This database is later updated by adding the SL training results obtained from the outdoor experiments in the hybrid navigation mode. When compared to the reference solution interpolated from the GPS/IMU solution for the micro-switch time events, the resulting KBS-based SL values obtained from both the ANN and FL showed similar accuracy of the predicted SL values with the mean (std) equal to 0 cm (4 cm). As a result, the SL obtained this way was subsequently integrated with the calibrated magnetometer heading (epoch-by-epoch EKF calibration) to reconstruct the trajectory. Fig. 7 shows the DR trajectory reconstruction. The original trajectory is plotted in blue, and the DR trajectories reconstructed by SL-Fuzzy and SL-ANN and the calibrated magnetometer heading are plotted in red and green. The DR trajectories represent the impact of SL prediction error and calibrated magnetometer heading error, as already explained.

The largest deviation of the DR trajectory can be observed at the upper part of the trajectory, where the user was walking around a car. In fact, since the magnetometer was earlier exposed to the environment with no cars (lower part of the trajectory), its calibration parameters were also estimated by the magnetic fields sensed on that part of the trajectory. Then, when the sensor approaches the car, the magnetometer heading starts to deviate due to the hard-iron distortion.

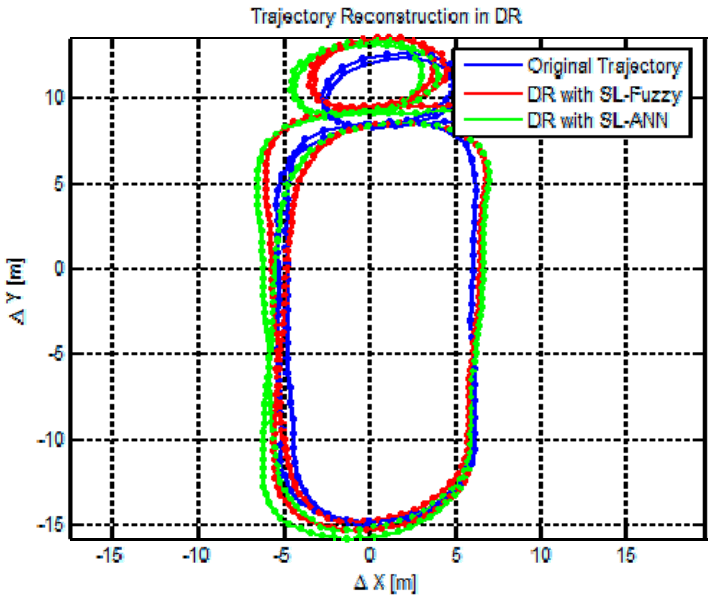

Fig. 7: Point-to-point DR trajectory reconstruction

This deviation indcates that the magnetometer compass heading modeling, as shown in (3), requires more time to adjust to the new local magnetic disturbance. Also, this deviation confirms that the magnetometer is noticeably affected by metal objects in its surroundings. Consequently, it is expected that the calibration parameters of the magnetometer may not have adequate accuracy to determine SD, once the user arrives at the building where there are many objects which can cause hard-iron and soft-iron distortions.

The statistical results of the outdoor calibration experiment, as shown in Table I, indicate a comparable performance of the SL modeling and ultimately in trajectory reconstruction of the ANN KBS and FL KBS. The 187m trajectory was reconstructed point-to-point with a CEP (50%) less than 2m, meeting the accuracy requirements of the system.

Note that the CEP (50%) is defined here somewhat loosely. Since sufficiently large number of test trajectories is not available at this point to define the CEP based on the misclosures of a representative sample of trajectories, in these tests each navigation step is treated as a "sample", and used to compute it's residual with respect to the reference trajectory. These samples are subsequently used to determine the 50% threshold that is reported here.

TABLE I
STATISTICAL FIT TO REFERENCE TRAJECTORY OF DR TRAJECTORIES GENERATED USING THE CALIBRATED MAGNETOMETER HEADING AND SL PREDICTED WITH BOTH FL AND ANN.

Test data set	SL model	Mean [m]	Std [m]	Max [m]	End Misclosure [m]	CEP (50%) [m]
187 m	FL	1.74	0.93	4.14	2.19	1.46
	ANN	2.05	1.06	4.53	3.01	1.97

B. *DR-KF Performance*

After performing an outdoor calibration process, and running in the hybrid navigation mode to tune the filter and update the KBS, the system was ready to perform navigation in a more challenging environment. For the outdoor experiments, where the magnetometer and the entire system were less affected by the ambient disturbances, (e.g. the scenario in which a single car caused heading deviation, and therefore the trajectory disturbance was rather moderate, as compared to the indoor environment) the SD value was not supervised by the DR-KF algorithm. But it was expected that in indoor environments, the SD would be subject to larger point to point deviations, due to more severe magnetic disturbances. Therefore, the main objective of the next test was to evaluate the system's performance in terms of KBS-SD modeling, DR-KF performance, as well as the trajectory reconstruction.

For this purpose, a part of the data collected on Aug 26, 2007, by operator E, was selected. The operator entered the building after about 20 minutes of calibration and hybrid navigation, and walked one and half indoor loops for about 97m in 2 minutes. As was discussed in Section 4.B, four different heading solutions based on magnetometer/gyro sensors are available. As an example, Fig. 8 shows a part of the trajectory solution; note that the remaining part of the trajectory demonstrates the KBS performance similar to that, plotted in Fig. 8.

The first heading solution is obtained from the multisensor GPS/IMU/magnetometer compass solution. In the absence of GPS signals, this solution is derived on the basis of the last calibration parameters applied to the gyro and magnetometer compass measurements. The second solution is obtained from the calibrated magnetometer compass, based on the last calibration provided by EKF. As can be seen in Fig. 8, this solution, in comparison to the first solution, is not sufficiently accurate most of the times, with a deviation of more than ±10º. The third solution is reconstructed using the gyro heading. For this solution, using the initial attitudes (from the last outdoor solution) and rate gyro, the angular rates are integrated over time, assuming that the gyro drifts do not change during integration. The last heading solution is reconstructed using the DR-KF module. In this solution, as was explained in Section 4.C, the SD value was decomposed into two variables, heading and heading rate. These values are then predicted based on the walking locomotion pattern (7), and updated based on the observation values, obtained from the integration of gyro and magnetometer (as explained in Section 4.B).

On the basis of this strategy, if the difference between the actual measurement and the predicted measurement, called the innovation, is more than a pre-defined threshold, this observation will be considered an outlier. The empirically selected threshold used for this dataset range between 3º and 5º, although the optimum threshold should be determined based on the locomotion pattern. Applying this threshold to the DR-KF results in outlier rejection, and observation replacement by the predicted measurement values.

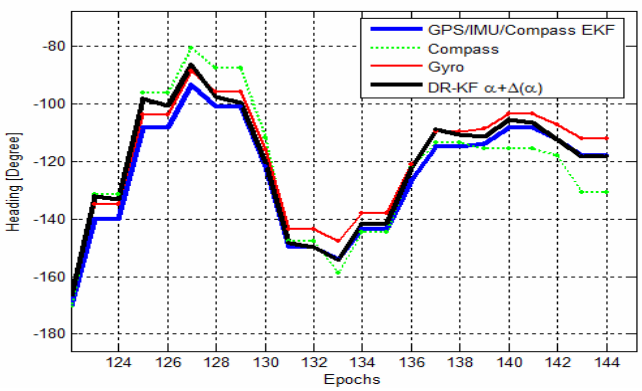

Fig. 8: KBS-based heading solutions; Δ(α) stands for $\frac{\dot{\alpha}}{2}\Delta t$

The heading solution obtained this way was subsequently integrated with the KBS-based FL SL modeling in the same DR-KF to reconstruct the trajectory. Fig. 9 shows the DR-KF trajectory reconstruction. The navigation solution obtained from DR-KF performs better than the point-to-point trajectory reconstruction because it is recreated by a dynamic model. As shown in Table II, the statistical results of the reconstructed trajectory based on DR-KF show an improvement of more than 20% in comparison to the point-to-point strategy, and most of the improvement comes from adjusting the SD value (see Fig. 8, which shows the prediction of heading).

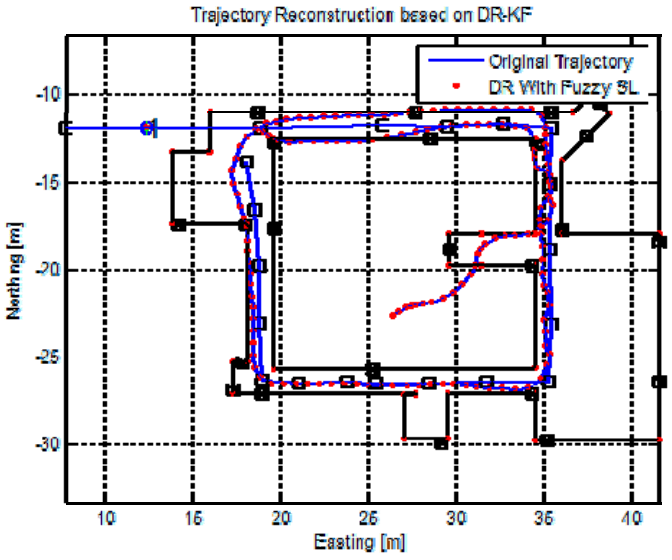

Fig. 9: Center for Mapping floor plan and DR-KF trajectory reconstruction based on FL SL modeling integrated with gyro and magnetometer heading.

TABLE II
STATISTICAL FIT TO REFERENCE TRAJECTORY OF DR TRAJECTORIES GENERATED USING POINT-TO-POINT STRATEGY AND DR-KF MODULE, WITH THE INTEGRATION OF GYRO AND MAGNETOMETER COMPASS HEADING.

Test data set	SL model	Mean [m]	Std [m]	Max [m]	End Misclosure [m]	CEP (50%) [m]
97 m One and half indoor loops	Point-to-point	1.30	0.94	2.55	2.74	1.19
	DR-KF	0.96	1.31	2.43	2.73	0.54

C. *Indoor/Outdoor Performance*

This part of the experiment is an attempt to evaluate the system's performance in the combination of both outdoor and confined environments. The 327m track, walked by operator E, includes two outdoor loops, followed by two loops inside the building. The indoor data of about 3 minutes in duration followed a 6-minute outdoor calibration and hybrid navigation period. Fig. 10 illustrates the DR-KF trajectory reconstruction using ANN SL modeling and FL SL modeling, with the source of heading depending on the GPS availability. For the outdoor performance, the epoch-by-epoch updated magnetometer compass heading was used, and for the indoor experiment, the heading was derived based on the last calibration parameters estimated for the gyro and magnetometer before entering the building. The statistical results, listed in Table III, confirm that the overall performance is viable within the 3-5 m CEP constraint. However, in general, the performance of KBS based on the ANN was more accurate than the FL approach.

D. *Indoor Limit Test Performance*

In the previous experiments, the DR-KF performance was tested for trajectories with limited length and short duration, particularly in the challenging environment. Since the system is expected to have time/distance limitations during prolonged GPS gaps, the question that needs to be answered is: how long the system can last in a challenging environment before it requires re-calibration? The data for this analysis include four loops of indoor navigation, which covers moderately changing locomotion dynamics, including turning at sharp corners, climbing a few stairs (see Fig. 1), and walking at different speeds. Operator S enters the building after ~30 minutes of outdoor maneuvering, so the EKF, the KBS for SL and SD modeling, and the entire system were all properly tuned. The indoor test duration lasted for about 6.5 minutes.

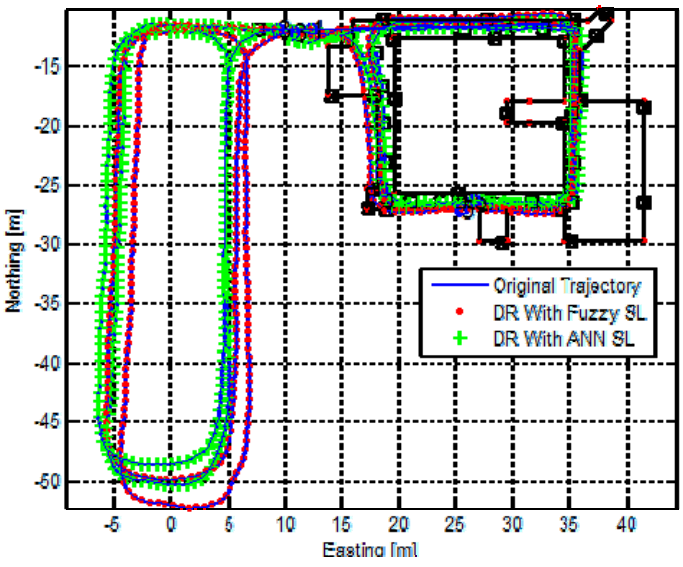

Fig. 10: Center for Mapping floor plan and DR reconstruction for FL SL modeling and ANN SL modeling, with epoch-by-epoch updated magnetometer compass heading (outdoor) and the integration of gyro and magnetometer compass heading (indoor).

TABLE III
STATISTICAL FIT TO REFERENCE TRAJECTORY OF DR TRAJECTORIES GENERATED USING SL PREDCITED WITH FL AND ANN, WITH EPOCH-BY-EPOCH UPDATED MAGNETOMETER COMPASS HEADING (OUTDOOR) AND THE INTEGRATION OF GYRO AND MAGNETOMETER COMPASS HEADING (INDOOR).

Test data set	SL model	Mean [m]	Std [m]	Max [m]	End Misclosure [m]	CEP (50%) [m]
327 m 2 indoor loops	FL	1.57	1.78	4.66	3.32	2.94
	ANN	1.15	1.57	4.52	2.60	2.53

Although more than six consecutive loops were made inside the building for this dataset, only four of them are used in this test. The last two loops were performed after the mobile user climbed up and down a few steps, and since at the current stage of implementation the stairs are not property handled yet in our KBS implementation, the last two loops are omitted here. Fig. 11 displays the DR-KF reconstruction for ANN SL modeling (top) and FL SL modeling (bottom), with the integration of gyro and magnetometer heading adjusted by the DR-KF. After each loop, the user remained stationary at a known marked point, where the system was assisted by a static ZUPT calibration. Table IV summarizes the statistics of the 261m reconstructed trajectory for the sample case, fitting the computed trajectory generated with SL predicted by both the FL and the ANN approach, and the heading adjusted by DR-KF, to the known reference trajectory, in order to quantify the overall DR navigation accuracy. The statistics in Table IV can be analyzed in three parts: the KBS-predicted SL, SD determination, and DR-KF structure. First, based on the 327-step trajectory (in 261 m) it can be concluded that the KBS SL modeling in the form of ANN and FL works properly.

However, for this dataset, the system performance with ANN SL was better than FL SL modeling, because the ANN SL-database developed earlier was mainly based on operator S data. Second, more than 16 sharp-turning corners were successfully traveled; that was fully supported by the tactical quality of HG1700 gyro. The magnetometer compass was also able to track the direction, but it was usually off by several degrees, especially when turning corners (e.g., as seen in Fig. 8). Third, the mechanism of DR-KF was partially tested in terms of controlling the DR parameters and reconstructing the trajectory. Several inaccurate SD values were rejected and replaced with the predicted value. However, because of the practically unchanged locomotion pattern in this dataset, it was not possible to completely evaluate the performance of the DR-KF.

As a conclusion, the overall performance of the system in the four tests presented here indicates that the PN system can navigate for more than 6 minutes with no GPS support and still remain within 5 m CEP (according to the approximated definition of CEP, as already explained), indoor and outdoor. However, the main limitation in the PN performance in DR mode is the SD determination. If the duration of a GPS outage is prolonged, the gyro heading solution is degraded resulting in unacceptable navigation accuracy. This performance assessment is not fully completed yet, especially for challenging environments, and more tests are required to address this issue.

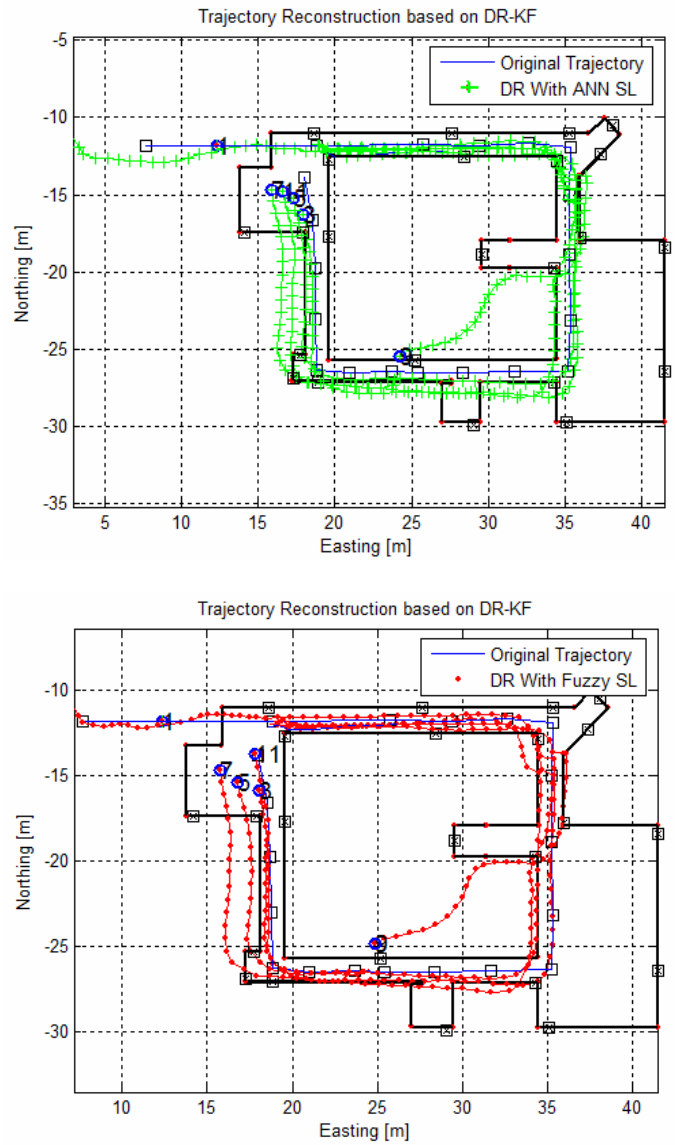

Fig. 11: Center for Mapping floor plan and DR-KF reconstruction for ANN SL-modeling (top) and FL SL-modeling (bottom), with the integration of gyro and magnetometer compass heading adjusted by DR-KF module.

TABLE IV
STATISTICAL FIT TO REFERENCE TRAJECTORY OF DR TRAJECTORIES GENERATED USING SL PREDCITED WITH FL AND ANN, AND THE INTEGRATION OF GYRO AND MAGNETOMETER COMPASS HEADING ADJUSTED BY THE DR-KF MODULE.

Test data set	SL model	Mean [m]	Std [m]	Max [m]	End Misclosure [m]	CEP (50%) [m]
261 m 4 indoor loops	FL	5.52	4.93	4.96	4.64	4.63
	ANN	5.78	4.41	5.05	4.50	4.53

6. CONCLUSION AND FUTURE WORK

The DR module of a PN supported by adaptive KBS was designed and implemented based on the off-the-shelf hardware technology. The experimental data have been collected by a tactical grade IMU, a relatively high-stability barometer, and a good quality magnetometer compass integrated with double difference GPS carrier phase observations. The objective of the DR navigation in this project was to: (1) determine the dynamic locomotion pattern, (2) utilize the KBS for accurate prediction of the SL, (3) calibrate the magnetometer compass and gyro to provide SD, and (4) develop a KBS in the form of a Kalman filter (DR-KF) to control and integrate the DR parameters, as well as to reconstruct the trajectory. The main limitation of the system was determined as the SD quality in confined environments.

The limitations of the system were tested by analyzing the system outdoor, indoor, and in a combination of both environments. It was determined that for more than four indoor loops, where the user walked 261m in about 6.5 minutes, the DR performance still met the required specifications, with the CEP within the required 3-5 m range. However, more tests are underway and more complex paths, including stairways, must be considered.

ACKNOWLEDGMENT

This research is supported by the National Geospatial-Intelligence Agency 2004 NURI grant.

REFERENCES

[1] D.A. Grejner-Brzezinska, C.K. Toth, Y. Jwa, and S. Moafipoor, "Seamless and reliable personal navigator," Proceedings, ION Technical Meeting, Monterey, CA, CD ROM, pp. 597-603, January 2006.

[2] D.A. Grejner-Brzezinska, C.K. Toth, S. Moafipoor, Y. Jwa and J. Kwon, "A low cost multi-sensor personal navigator: system design and calibration," Presented at IEEE/ION PLANS Meeting, San Diego, CA, April 2006.

[3] D.A. Grejner-Brzezinska, C.K. Toth, S. Moafipoor, and Y. Jwa, "Multi-sensor personal navigator supported by human motion dynamics model," Proceedings, 3rd IAG Symposium on Geodesy for Geotechnical and Structural Engineering/12th FIG Symposium on Deformation Measurements, Baden, Austria, CD ROM, May 2006.

[4] D.A. Grejner-Brzezinska, C.K. Toth, and S. Moafipoor, "Adaptive knowledge-based system for personal navigation in GPS-denied environments," Proceedings, ION National Technical Meeting, January 22-24, San Diego, CA, CD ROM, pp.517-521, January 2007.

[5] D.A. Grejner-Brzezinska, C.K. Toth, S. Moafipoor, "Pedestrian tracking and navigation using adaptive knowledge system based on neural networks and fuzzy logic," *Journal of Applied Geodesy*, vol. 1, No. 3, pp. 111-123, 2007, invited.

[6] C.K. Toth, D.A. Grejner-Brzezinska, S. Moafipoor, "Pedestrian tracking and navigation using neural networks and fuzzy logic," Proceedings, IEEE International Symposium on Intelligent Signal Processing, Alcala De Henares, Madrid, Spain, CD ROM, pp. 657-662, October 2007.

[7] S. Moafipoor, D.A Grejner-Brzezinska, and C.K. Toth, "A fuzzy dead reckoning algorithm for a personal navigator," Proceedings, ION GNSS Meeting, Fort Worth, Texas, CD-ROM, 2007, pp.48-59, September 2007, in review for *Navigation*.

[8] E. Foxlin, "Pedestrian tracking with shoe-mounted inertial sensors," *IEEE Computer Graphics and Application*, vol. 25, No. 6, 2005, pp.38-46.

[9] S. Moafipoor, D.A Grejner-Brzezinska, and C.K. Toth, "Adaptive calibration of a magnetometer compass for a personal navigation system," Proceedings, International Global Navigation Satellite Systems Society (IGNSS) Symposium, the University of New South Wales, Sydney, Australia, CD ROM, December 2007.

[10] D.A Grejner-Brzezinska, C.K. Toth and S. Moafipoor, "Adaptive knowledge based system based on artificial neural networks and

fuzzy logic for pedestrian navigation," Proceedings, International Global Navigation Satellite Systems Society (IGNSS) Symposium, The University of New South Wales, Sydney, Australia, CD ROM, December 2007.

[11] D.A. Grejner-Brzezinska, C.K. Toth, S. Moafipoor and J. Kwon, "Multi-sensor personal navigator: system design and calibration," Proceedings, SMF/UPIMap, Seoul, Korea, CD ROM, October 2006.

[12] Wang, J.J., J. Wang, D. Sinclair, and L. Watts, "A neural network and Kalman filter hybrid approach for GPS/INS integration," Proceedings, 12th IAIN Congress & 2006 Int. Symp. On GPS/GNSS, Jeju, Korea, pp. 277-282, October 2006.

[13] C. Jekeli, *Inertial navigation systems with Geodetic applications,* Walter de Gruyter, New York, NY, USA, 2000.

[14] J. Crassidis, K. Lai, R. Harman, "Real-time attitude independent three-axis magnetometer calibration," *Journal of Guidance, Control, and Dynamics*, vol. 28, No. 1, 2005, pp. 115–120.

[15] B. Schaffrin, "Connecting the dots: the straight-line case revisited," *Deutscher Verein für Vermessungswesen (zfv2007)*, 132.Jg., 2007, pp. 385-394.

[16] J.M. Hausdorff, Y. Ashkenazy, C.K. Peng, P.C. Ivanov, H.E. Stanley, A.L. Goldberger, "When human walking becomes random walking: fractal analysis and modeling of gait rhythm fluctuations," *PHYSICA A*, vol. 302, 2001, pp.138-147.

[17] H. Ning, L. Wang, W. Hu, T. Tan, "Model-based tracking of human walking in monocular image sequences," TENCON '02. Proceedings, IEEE Region 10 Conference on Computers, Communications, Control and Power Engineering, Beijing, China, pp. 537-540, October 2002.

[18] M. Sugeno and G.T. Kang, "Structure identification of fuzzy model," *Fuzzy Set Syst*., vol. 28, No. 1, 1988, pp. 15-33.

[19] D. Simon, "Kalman filtering for fuzzy discreet time dynamic systems," *Applied soft computing*, vol. 3, No. 3, 2003, pp. 191-207.